Electron Correlation Resonances in the Transport through a Single Quantum Level

A. Levy Yeyati, A. Martín-Rodero, and F. Flores
Departamento de Física de la Materia Condensada C-XII, Facultad de Ciencias, Universidad Autónoma de Madrid, E-28049 Madrid, Spain
(Received 23 June 1993)

Correlation effects in the transport properties of a single quantum level coupled to electron reservoirs are discussed theoretically using a nonequilibrium Green function approach. Our method is based on the introduction of a second-order self-energy associated with the Coulomb interaction that consistently eliminates the pathologies of previous perturbative calculations. We present results for the current-voltage characteristic illustrating the different correlation effects that may be found in this system, including the Kondo anomaly and Coulomb blockade. We discuss the experimental conditions for the simultaneous observation of these effects in an ultrasmall quantum dot.

PACS numbers: 72.10.Bg, 72.15.Qm, 73.20.Dx, 73.40.Gk

The transport properties of a quantum dot coupled to electron reservoirs have received considerable attention in recent years from both the experimental [1] and the theoretical [2] sides. With the advent of nanotechnologies, an ideal experimental device where tunneling takes place through a single electronic level within the dot is now feasible. Different theoretical papers [3–6] have suggested that the tunneling through this single quantum level can be appropriately described by the Anderson Hamiltonian

$$H = \sum_{\sigma} \epsilon_0 n_{0\sigma} + \sum_{\nu,k,\sigma} T_k^{\nu} (c_{k\sigma}^{\nu\dagger} c_{0\sigma} + c_{o\sigma}^{\dagger} c_{k\sigma}^{\nu}) + \sum_{\nu,k,\sigma} (\epsilon_k^{\nu} + \mu^{\nu}) n_{k\sigma}^{\nu} + U n_{0\uparrow} n_{0\downarrow}, \quad (1)$$

where ϵ_0 represents the quantum dot level, U is the effective Coulomb repulsion within the dot, $\epsilon_k^{\nu} + \mu^{\nu}$ with $\nu =$ left or right denotes the reservoir single-particle energies, $\mu^L - \mu^R = eV$ being the applied bias, and T_k^{ν} the coupling between the reservoir states and the quantum dot level.

The Hamiltonian (1) is expected to describe the main correlation effects associated with the quantum dot. In particular, a Kondo-like resonance near the Fermi energy should be reflected in the current-voltage characteristic at low voltages, when the dot level is nearly half filled. On the other hand, a Coulomb blockade effect should lead to a reduction in the conductance up to voltages large enough to overcome the Coulomb repulsion in the dot level. Previous theoretical efforts have been concerned mainly with one of these two effects. In Refs. [3–5,7] the Kondo effect is studied using a variety of techniques in both the linear and nonlinear regimes, whereas the charging effects have been analyzed in Refs. [6,8]. The aim of this paper is to present a solution for this model which would allow us to describe accurately all the physically relevant regimes, showing how many-body resonances appear in the current-voltage characteristic. We pay particular attention to the situation where features related to the Kondo and charging effects may be found simultaneously. Based on these results, we shall also discuss in detail the experimental conditions necessary to observe those resonances in semiconductor nanostructures.

The transport properties of this model can be analyzed by using the Keldysh formalism [9], where the retarded, G^r, and the distribution, G^{+-}, Green functions are defined as follows:

$$G_{i,j}^r(w) = -i \int \theta(t) \langle c_j^{\dagger}(t) c_i(0) + c_i(0) c_j^{\dagger}(t) \rangle e^{iwt}\, dt\,, \quad (2)$$

$$G_{i,j}^{+-}(w) = i \int \langle c_j^{\dagger}(t) c_i(0) \rangle e^{iwt}\, dt\,.$$

These Green functions can be calculated by starting with the L and R reservoirs decoupled from the dot level. This case defines the unperturbed Green functions $\mathbf{G}^{(0)}(w)$. Then $\mathbf{G}(w)$ can be obtained by coupling the dot level to the reservoirs and by introducing the self-energies $\mathbf{\Sigma}^r$ and $\mathbf{\Sigma}^{+-}$ which take into account the Coulomb correlations within the dot. Once the different Green functions are obtained from the corresponding Dyson equations [9], the current intensity I_ν between reservoir ν and the dot level is given by

$$I_\nu = \frac{2e}{\hbar} \sum_k T_k^{\nu} \int dw [G_{k,0}^{\nu+-}(w) - G_{0,k}^{\nu+-}(w)]. \quad (3)$$

The crucial point in order to solve this problem is to find a reasonable approximation for the self-energies. For $U = 0$, $\mathbf{\Sigma} = 0$ and the exact $\mathbf{G}(w)$ can be easily obtained using conventional Green function techniques [10].

The effect of a finite U can be included by using perturbation theory in U. This perturbative approach has been extensively analyzed by Yoshida and Yamada [11] and Zlatic and Horvatic [12] (hereafter referred to as YY and ZH) for the equilibrium Anderson model (zero applied bias). Hershfield *et al.* [3] have extended this approach to the nonequilibrium case by calculating $\Sigma_{0\sigma}^r(w)$ and $\Sigma_{0\sigma}^{+-}(w)$ up to second order in U.

In the YY and ZH approach, $\Sigma_{0\sigma}^{(2)}(w)$ is calculated from

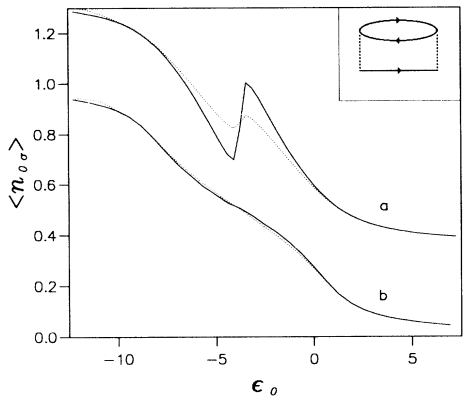

FIG. 1. Fulfillment of the Friedel-Langreth sum rule as a function of the dot level position using the second-order self-energy as calculated: (a) starting from the Hartree-Fock solution and (b) imposing self-consistency in the dot level charge. The full line corresponds to the dot level charge $\langle n_{0\sigma}\rangle$ and the dotted line corresponds to $-\frac{1}{\pi}\eta(0)$. Inset: Second-order diagram used to calculate the self-energies.

the second-order diagram shown in Fig. 1 (inset), where each Green function line is a Hartree-Fock dressed propagator, whose retarded part is given by

$$G^{r\mathrm{HF}}_{0\sigma}(w) = \frac{1}{w - \bar{\epsilon}_{0\sigma} + i\Gamma_L(w) + i\Gamma_R(w)}, \tag{4}$$

where $\bar{\epsilon}_{0\sigma} = \epsilon_0 + U\langle n_{0\bar{\sigma}}\rangle$ and $\Gamma_\nu = 2\pi\sum_k \mid T^\nu_k \mid^2 \times\delta(w-\epsilon_k)$.

Although this approximation gives a good description of the electron correlation effects in the symmetric case ($\epsilon_0 = -U/2$), it presents some drawbacks when one moves away from this condition. In the equilibrium case this is clearly illustrated by the failure of the Friedel-Langreth [13] (hereafter referred as FL) sum rule that relates the "impurity" charge $\langle n_{0\sigma}\rangle$ to the phase shift created by the impurity at the Fermi energy $\eta(0) = \mathrm{Im}\,[\ln G^r_{0\sigma}(0)]$.

Figure 1(a) shows the degree of fulfillment of the FL sum rule, $\langle n_{0\sigma}\rangle = -\frac{1}{\pi}\eta(0)$, using the second-order self-energy $\Sigma^{r(2)}_{0\sigma}(w)$ in the YY-ZH approach. In this figure we compare $\langle n_{0\sigma}\rangle$ with $-\frac{1}{\pi}\eta(0)$ as a function of the dot level ϵ_0, for $U/\Gamma = 2.4\pi$, neglecting the frequency dependence in Γ_ν, and taking $\Gamma_L = \Gamma_R = \Gamma/2$.

Improvements over the above $\Sigma^{(2)}_{0\sigma}$ are not easy to obtain. For instance, one could insert the full self-consistent dressed propagators instead of the Hartree-Fock ones for calculating the diagram in Fig. 1. This sort of self-consistent perturbation theory is charge conserving [14] and would verify the FL sum rule. However, it has been shown that it leads to a poorer description of the quasiparticle spectral density [15].

Our proposal to improve the YY and ZH approach is the following: Instead of using the Hartree-Fock solution as the initial one-electron problem for the calculation of $\Sigma^{(2)}_{0\sigma}$, we use a different self-consistent field as a starting point. In this initial one-electron problem the Hartree-Fock level, $\bar{\epsilon}_{0\sigma}$, in Eq. (4) is replaced by an effective level $\epsilon_{\mathrm{eff}\sigma}$, which is determined by imposing self-consistency between the initial and final dot level occupancies. As shown in Fig. 1(b), this way of calculating the second-order self-energy gives a solution that closely verifies the FL sum rule.

Notice that this procedure is formally correct within perturbation theory: We have decomposed $H = H_{\mathrm{eff}} + V$, where H_{eff} is the one-electron part of Hamiltonian (1) with ϵ_0 replaced by $\epsilon_{\mathrm{eff}\sigma}$, and we treat $V = H - H_{\mathrm{eff}}$ as a perturbation. The fulfillment of the FL sum rule and the condition of charge consistency provide an appealing interpretation for $\epsilon_{\mathrm{eff}\sigma}$: It must behave like $\epsilon_0 + \mathrm{Re}\Sigma^r_{0\sigma}(0)$, the effective potential at the Fermi energy. Obviously, for the symmetric case our approach coincides with that of YY and ZH.

This procedure allows us to get a good description of the Kondo-like peak appearing around the Fermi energy and the overall behavior of the spectral density for a broad range of parameters (ϵ_0, U/Γ). However, for high values of U/Γ and far from the symmetric situation, the position and the spectral weights of the resonances around ϵ_0 and $\epsilon_0 + U$ are not so well described [16]. The reason is that $\Sigma^{r(2)}_{0\sigma}$ does not yield the atomic limit when $w \sim U \gg \Gamma$. To improve the solution given above in this region we introduce the following self-energy [16]:

$$\Sigma^r_{0\sigma}(w) = \frac{\Sigma^{r(2)}_{0\sigma}(w)}{1 - \alpha\Sigma^{r(2)}_{0\sigma}(w)}, \tag{5}$$

with

$$\alpha = \frac{(1 - \langle n_{0\bar{\sigma}}\rangle)U + \epsilon_0 - \epsilon_{\mathrm{eff}}}{\langle n_{0\bar{\sigma}}\rangle(1 - \langle n_{0\bar{\sigma}}\rangle)U^2},$$

which has the virtue that it yields the appropriate atomic limit [16,17], for $w \sim U$ and $\Gamma/U \to 0$, and behaves like $\Sigma^{r(2)}_{0\sigma}$ for $U/\Gamma \to 0$.

Let us now turn our attention to the nonequilibrium situation. For the sake of simplicity, we shall assume that in Eq. (1) $\mu^L = -\mu^R = eV/2$. Following our approach for the equilibrium Anderson model, we obtain the different nonequilibrium self-energies, $\Sigma^r_{0\sigma}$ and $\Sigma^{+-}_{0\sigma}$, by introducing the effective levels $\epsilon_{\mathrm{eff}\sigma}$, μ^L_{eff}, and μ^R_{eff} in the initial one-electron Hamiltonian

$$H^{(\mathrm{transport})}_{\mathrm{eff}} = \sum_\sigma \epsilon_{\mathrm{eff}\sigma} n_{0\sigma} + \sum_{\nu,k,\sigma} (\epsilon^\nu_k + \mu^\nu_{\mathrm{eff}}) n^\nu_{k\sigma} + \sum_{\nu,k,\sigma} T^\nu_k (c^{\nu\dagger}_{k\sigma} c_{0\sigma} + c^\dagger_{0\sigma} c^\nu_{k\sigma}). \tag{6}$$

As a natural extension of our procedure for the equilibrium case, $\epsilon_{\mathrm{eff}\sigma}$, μ^L_{eff}, and μ^R_{eff} are determined by imposing self-consistency in the dot level charge and in the currents I_L and I_R defined by Eq. (3).

Equation (6) allows us to calculate the one-electron Green functions $\mathbf{G}^{\mathrm{eff}}$ that will be used to obtain $\Sigma^{r(2)}_{0\sigma}$

and $\Sigma_{0\sigma}^{+-(2)}$ by means of a second-order perturbative calculation, and finally $\Sigma_{0\sigma}^{\zeta}(w)$ and $\Sigma_{0\sigma}^{+-}(w)$ by using the equivalent of Eq. (5) for the nonequilibrium case.

Let us remark that our method eliminates, in a natural way, the pathologies that arise when the perturbation is performed upon the Hartree-Fock solution. In the nonequilibrium case these pathologies are reflected in the unphysical behavior of the dot level charge as a function of ϵ_0 (around $\epsilon_0 \sim -U/2$); the currents I_L and I_R also exhibit unphysical features [3] including violation of current conservation ($I_L \neq I_R$). A detailed comparison of the results given by the different approaches, together with a more comprehensive discussion of our method, will be presented in a future publication.

In order to illustrate the kinds of results obtained by our method we have considered two different situations, with the dot level below (Fig. 2) and above (Fig. 3) the Fermi energy, respectively. In the second case the dot level is almost empty at zero bias.

Figure 2 shows the current intensity, I, and the differential conductance $g = \partial I/\partial V$, as a function of the applied bias, for $\epsilon_0 = -\pi$ and $U = 0$, $\pi/2$, π, 2π, and 4π, where all the energies hereafter are measured in units of Γ. Our results for g show a single broad peak around

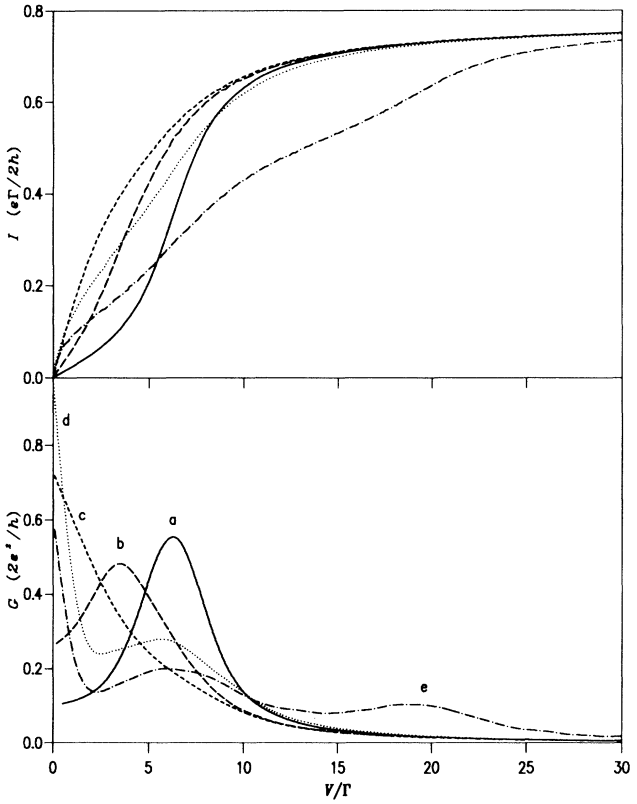

FIG. 2. Current I and differential conductance g obtained using our method for $\epsilon_0 = -\pi$ and $U = 0$ (a), $\pi/2$ (b), π (c), 2π (d), and 4π (e). All the energies are measured in units of the elastic decay rate at the dot Γ.

$V = 2\pi$ for $U = 0$; this corresponds to the dot level $\epsilon_0 = -\pi$ crossing the right reservoir chemical potential $\mu^R = -V/2$. For small U ($U < |\epsilon_0|$) this one-electron-like resonance is shifted and adopts a somewhat asymmetric shape. On the other hand, for large U (see case $U = 4\pi$ in Fig. 2) three different features are clearly present in the current-voltage characteristic. The conductance peak at $V = 0$ is related to the Kondo resonance appearing in the dot spectral density around the Fermi energy [3], while the peaks at $V = 2\pi$ and $V = 4\pi$ correspond to the crossing of the dot "ionization" and "affinity" levels, ϵ_0 and $\epsilon_0 + U$, with the reservoir's chemical potentials. We should comment that these two peaks reflect the charging effects associated with the dot level: The second level can only be filled when the applied bias overcomes the repulsion between the second and the first electrons. For the particular case $U = 2\pi$ we have a symmetric problem with the two dot levels crossing the left and right chemical potentials at the same bias, $V = 2\pi$, leading to a single "charging effect" peak. Notice that in this case the conductance at $V = 0$ reaches its maximum value $2e^2/h$. Finally, the case $U = \pi$ illustrates the transition between small and large U, with a new correlation structure arising due to the overlap between both Kondo and charging effects, the resonances merging into a broad peak around $V = 0$. This transition is also apparent in the current intensity $I(V)$ shown in Fig. 2, where the case $U = \pi$ defines the border between the highly correlated limit (Kondo and charging effects completely separated) and the one-electron-like behavior.

Figure 3 shows $I(V)$ and g as a function of V for $\epsilon_0 = 3\pi$ and $U = 0$, 2π, 4π, and 6π. In these cases the dot level is above the Fermi energy, and for $V = 0$ no Kondo-like peak appears in the spectral density of states. As before, the two peaks appearing in the differential conductance for $U \geq 2\pi$ are related to the filling of the ionization, ϵ_0, and affinity, $\epsilon_0 + U$, levels as a function of the applied voltage. As shown in Fig. 3(b), the voltage difference between the two peaks for $U \geq 2\pi$ is approximately equal to $2U$. On the other hand, the conductance peak at $V = 2\epsilon_0$ is reduced to nearly half its $U = 0$ value when the interaction increases. It is also worth noticing that the I-V curve in this case exhibits a steplike behavior which is more pronounced for increasing values of U. The relative height of these steps is in agreement with calculations based on a simple atomiclike model for the dot Green functions [8].

Figures 2 and 3 show the different kinds of current-voltage characteristics one gets for the single dot level described by Hamiltonian (1). For U sufficiently large, two resonances associated with the ionization and affinity levels can always be observed in the differential conductance. In this case correlation effects are very important, giving rise to an additional resonance at $V = 0$ when the ionization level is initially filled.

The results found in this paper suggest that the Kondo-

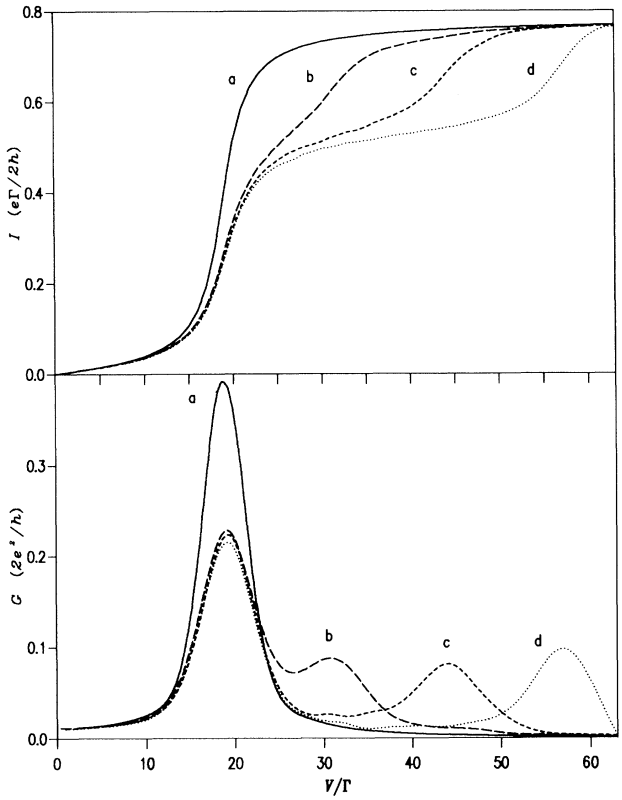

FIG. 3. Same as Fig. 2 for $\epsilon_0 = 3\pi$ and $U = 0$ (a), 2π (b), 4π (c), and 6π (d).

like resonance and the peaks associated with the charging effects of the quantum level could be found simultaneously in a quantum dot, provided that the temperature is sufficiently below the Kondo temperature. As an example, we consider a GaAs dot of size $L \sim 100$ Å both in the vertical and lateral directions, sandwiched between two GaAs wires and two AlGaAs barriers, as those studied in Ref. [18]. A single bound level around 50 meV is found by solving numerically a simple double barrier model with a barrier height ~ 300 meV. The parameter U can be evaluated as the Coulomb integral for the wave function corresponding to this bound level, which roughly yields $U \sim e^2/\epsilon L \simeq 15$ meV, in agreement with the dot classical capacitance energy [8]. Then, varying the AsGa wires doping around $10^{18}/\text{cm}^3$, one could get an experimental device close to some of the theoretical cases analyzed in Figs. 2 and 3. In particular, for $n = 10^{18}/\text{cm}^3$ and a barrier width of 30 Å, we find $\epsilon_0/\Gamma \simeq -3$ and $U/\Gamma \simeq 8$, not far from one of the cases presented in Fig. 2. We should recall that finite conduction band effects are not included in our present calculation; one should always keep in mind that for V sufficiently large the effect of the bottom edge of the semiconducting wires would be present in the I-V characteristic.

In conclusion, we have presented an accurate solution for the many-body problem of a single dot level between two biased reservoirs. Our results show the experimental conditions one should achieve to observe in the differential conductance a peak related to the Kondo-like structure in the density of states, and a complementary structure associated with the charging effects of the dot level. By adjusting appropriately the dimensions and the doping of a quantum semiconducting dot, we have shown how the different peaks could be determined by measuring the differential conductance.

Support by Spanish CICYT (Contract No. PB89-0165) is acknowledged. We also thank Dr. J. Ferrer, Professor J.P. Hernandez, and Professor S.Y. Wu for interesting discussions.

[1] M.A. Reed, J.H. Randall, R.J. Aggarwal, R.J. Matyi, T.M. Moore, and A.E. Wetsel, Phys. Rev. Lett. **60**, 535 (1988); U. Meirav, M.A. Kastner, and S.J. Wind, Phys. Rev. Lett. **65**, 771 (1990); B. Su, V.J. Goldman, and J.E. Cunningham, Phys. Rev. B **46**, 7644 (1992).

[2] C.W.J. Beenakker, Phys. Rev. B **44**, 1646 (1991); Y. Meir, N.S. Wingreen, and P.A. Lee, Phys. Rev. Lett. **66**, 3048 (1991).

[3] S. Hershfield, J.H. Davies, and J.W. Wilkins, Phys. Rev. Lett. **67**, 3720 (1991); Phys. Rev. B **46**, 7046 (1992).

[4] Y. Meir, N.S. Wingreen, and P.A. Lee, Phys. Rev. Lett. **70**, 2601 (1993).

[5] T.K. Ng, Phys. Rev. Lett. **70**, 3635 (1993).

[6] A. Groshev, T. Ivanov, and V. Valtchinov, Phys. Rev. Lett. **66**, 1082 (1991).

[7] T.K. Ng and P.A. Lee, Phys. Rev. Lett. **61**, 1768 (1988).

[8] L.Y. Chen and C.S. Ting, Phys. Rev. B **44**, 5916 (1991).

[9] L.V. Keldysh, Zh. Eksp. Teor. Fiz. **47**, 1515 (1964) [Sov. Phys. JETP **20**, 1018 (1965)]; L.P. Kadanoff and G. Baym, in *Quantum Statistical Mechanics* (Benjamin, New York, 1962).

[10] C. Caroli, R. Combescot, P. Nozières, and D. Saint-James, J. Phys. C **4**, 916 (1971).

[11] K. Yosida and K. Yamada, Prog. Theor. Phys. **46**, 244 (1970).

[12] V. Zlatic and B. Horvatic, Phys. Rev. B **28**, 6904 (1983).

[13] D.C. Langreth, Phys. Rev. **150**, 516 (1966).

[14] G. Baym, Phys. Rev. **127**, 1153 (1962).

[15] J.A. White, Phys. Rev. B **45**, 1100 (1992).

[16] A. Martín-Rodero, F. Flores, M. Baldo, and R. Pucci, Solid State Commun. **44**, 911 (1982); J. Ferrer, A. Martín-Rodero, and F. Flores, Phys. Rev. B **36**, 6149 (1987).

[17] J. Hubbard, Proc. R. Soc. London A **276**, 238 (1963); S. Doniach, Adv. Phys. **18**, 819 (1969).

[18] J.N. Randall, M.A. Reed, J.H. Luscombe, G.A. Frazier, W.R. Frensley, A.C. Seabaugh, Y.C. Kao, T.M. Moore, and R.J. Matyi, Proc. SPIE Int. Soc. Opt. Eng. **1284**, 66 (1990).